

This is a preprint of a paper intended for publication in a journal or proceedings. Since changes may be made before publication, the preprint is available with the understanding that it will not be cited or reproduced without the permission of the author.

UCRL - 76937  
PREPRINT

Conf - 751116-10



LAWRENCE LIVERMORE LABORATORY  
University of California/Livermore, California

Bio-Medical Division

A HIGH-EFFICIENCY MULTIDETECTOR SYSTEM FOR TUMOR SCANNING

J. A. Kirby, P. L. Phelps, G. A. Armantrout, and D. Sawyer  
R. N. Beck

November 18, 1975

NOTICE  
This report was prepared at an account of work sponsored by the United States Government. Neither the United States nor the Lawrence Livermore Laboratory Research and Development Administration, nor any of their contractors, nor any of their subcontractors, nor any of their employees, makes any warranty, express or implied, or assumes any legal liability or responsibility for the accuracy, completeness or usefulness of any information, apparatus, product or process disclosed, or represents that its use would not infringe privately owned rights.

This paper was prepared for submission to  
"BEE 1975 Nuclear Science Symposium  
San Francisco, California, November 17-20, 1975

112

# A HIGH-EFFICIENCY MULTIDETECTOR SYSTEM FOR TUMOR SCANNING

J. A. Kirby, P. L. Phelps, C. A. Armantrout, and D. Sawyer  
Lawrence Livermore Laboratory, University of California  
Livermore, California 94550

and

R. N. Beck  
The Franklin McLean Memorial Research Institute  
The University of Chicago  
Chicago, Illinois 60637

## Summary

A high-efficiency detector system developed especially for medical imaging has three specially cut Ge(Li) coaxial detectors (total volume 249 cm<sup>3</sup>). At 122 keV, the peak efficiency is 93% of that of a 7.6 x 7.6 cm NaI(Tl) detector. Degradation of the parallelized energy resolution is avoided and resolution is improved by 35% over that of conventional output-summing techniques by gating the detector outputs. In effect this multiplexes them to a single line output.

## Introduction

It is well known that solid-state detectors give better energy resolution than NaI(Tl) detectors, but the low relative efficiencies of the available solid-state detectors prohibits their use for many applications. This is the case in medical imaging, particularly for brain tumor-scanning where the patient receives an injection of a radioisotope solution (usually <sup>99m</sup>Tc, 140 keV). Solid-state detectors would give better energy resolution and thus better image quality than the conventional NaI(Tl) detectors in use, but both the scanning time and radioisotope dose would have to be increased to impractical levels to offset the loss in detector efficiency. A Ge(Li) detector system was needed with its characteristic good energy resolution but with efficiencies, especially at 140 keV, comparable to those of a 7.6 x 7.6 cm NaI(Tl) detector. To achieve this result, a multidetector system was built to include three specially cut coaxial Ge(Li) detectors having a total summed volume of 249 cm<sup>3</sup> with a detector surface area of approximately 83 cm<sup>2</sup>. To fulfill the need for the best possible resolution, an electronic gating system was designed to parallel the detectors. This circuit in effect multiplexes the three detectors to a single line output. The result is an overall energy resolution that approximately equals the average energy resolution of the three detectors rather than the square root of the sum of the squares of the individual detector resolutions that is obtained with direct summing of the detector signals.

Our purpose here is to describe the system and to present performance data to illustrate its efficiency, resolution, and other parameters.

## Detectors And Cryostat

A major objective in constructing the detector was to fill a cylinder 10 cm in diameter by 3 cm thick with active detector material so as to make optimum use of the available 10-cm multihole focused collimators at the University of Chicago. Since this size is considerably larger than the available detector-quality germanium ingots, our approach was

based on detectors operating in parallel.

Since high packing density was desired for the detector system, a square "coaxial" detector geometry was chosen. Figure 1 shows the cross section of the detector delineating the junction edges. Also shown is the way in which the detectors were mounted in the cryostat to achieve an active volume 10 cm in diameter and 3 cm thick.

The detectors were fabricated from relatively inexpensive horizontally grown germanium. The configuration was that of a simple open-ended coaxial detector, and fabrication and mounting of the detectors followed standard Ge(Li) procedures. The signal leads from the three detectors were brought out through three separate feed-throughs so that all the electronics would be external to the cryostat (Fig. 2).

The cryostat was fabricated from stainless steel and has a beryllium window. The vacuum is maintained by an internal sorption-type pump mounted on the cold finger and a drip-type liquid-nitrogen dewar is used. All components were ruggedized to withstand the accumulative forces anticipated in the operation of the rectilinear scanner.

## Electronics

Figure 2 is a block diagram of the electrical system and Fig. 4 shows the system schematics. Each detector has its own preamplifier, shaping amplifier, discriminator, and timing units. Common to all the detectors are the gating logic, analog gates, and buffer amplifier. The buffer amplifier output is connected to ten single-channel analyzers when scanning; otherwise a multichannel analyzer is connected to check the detector performance.

The basic operation of the system can be described as follows. The output from each preamplifier, besides being connected to a shaping amplifier, is connected to a leading-edge timing unit. Each timing unit has a one-shot output that is initiated by a detector pulse when a preset threshold level is exceeded. The duration of the pulse is preset according to the risetime of the shaping amplifier output (a one-shot duration of about 6  $\mu$ sec for a shaping time constant of 2  $\mu$ sec). The pulse width is not critical but it must be long enough to end sometime after the pulse peak (Fig. 5).

These one-shot outputs are sent to three type-D flipflops (clocked at 4.5 MHz), which are used to synchronize the data input to the sequential logic (Fig. 6). This logic, upon sensing an input from a detector, generates an output pulse for the appropriate detector channel based upon behavior to be discussed later. This output pulse is of the same

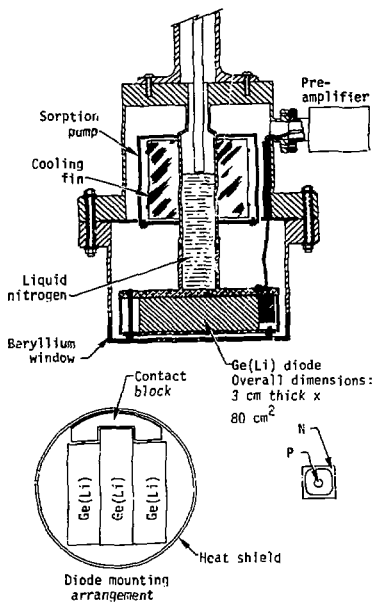


Fig. 1. Cross-section diagram of the cryostat and detector assembly.

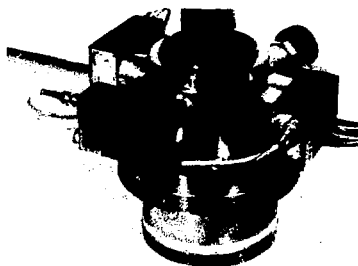


Fig. 2. External view of the detector assembly.

duration as the one-shot output  $\pm 2$  clock periods. Note: the gating logic output can generate only one pulse at any time although it has three separate output lines, one for each detector.

The shaped amplifier outputs are sent to a three-channel analog gate (virtual ground type) and are gated by the gating logic pulse into an XI buffer amplifier.

#### Time Pickoff Unit

The preamplifier pulse is sent to the timing unit where, after differentiation and amplification, a comparator acts as a lower-level discriminator. This discriminator was set to about  $50 \text{ mV}$  (that is,  $60 \text{ keV}$ ) for normal operation, with the threshold adjustment brought out to the front panel. This discriminator serves to prevent triggering of the one-shots by noise or by pulses below the energy of interest.

#### Gating Logic Unit

The gating logic operates in a fully synchronized manner, and uses a completely specified state-counter controller. The operation of this can be explained with the aid of a state-to-state diagram (Fig. 7; see also Fig. 6). The four possible states of the machine are represented by the circled letters  $a$ ,  $b$ ,  $c$ , and  $d$ . The zero or reset state of the machine (state  $a$ ) represents the condition when no pulses from one-shots are present. States  $b$ ,  $c$ , and  $d$  indicate servicing of the #1, #2, or #3 detectors, respectively. The actual state of the machine is equivalent to the binary state of the two controller flip-flops  $P$  and  $S$ .

In the case of coincidence within the input sampling period, the output is governed on the basis of priority; detector priority is assigned in ascending order of detector number. Other logical behavior schemes could have been designed into the logic to deal with coincidence, but this priority scheme was chosen because of design simplicity and ease of checkout.

Assume that the logic is in state  $a$  with no input pulses. If the  $1'$  input comes up either alone or in coincidence with  $2'$  and  $3'$ , the logic will go to state  $b$ , and output 1 will turn on. Once in state  $b$ , logic output 1 will be on as long as  $1'$  is on, regardless of the state of inputs  $2'$  and  $3'$ . After the  $1'$  input has ceased, the logic no longer generates the 1 output but remains in state  $b$  until inputs  $2'$  and  $3'$  are clear, at which time the logic returns to state  $a$ . This ensures that no output will be generated except at the beginning of the one-shot input. Otherwise, the analog gate could be turned on in the middle of a shaped pulse, thereby passing a distorted detector pulse to the multichannel analyzer. The same analysis applies to servicing the #2 and #3 detectors except for the priority decision in the case of coincidence.

#### Panel Features

The electronics, except for the preamplifiers and the shaping amplifiers, is contained in one triple-width NIH bin module (Fig. 8). The front panel has adjustments for the discriminators and a scope jack for each one-shot. Three three-position switches permit control of each channel of the analog gate for on all the time, off all the time, or gated. This permits easy setup and checkout of each channel with a multichannel analyzer and scope. The binary

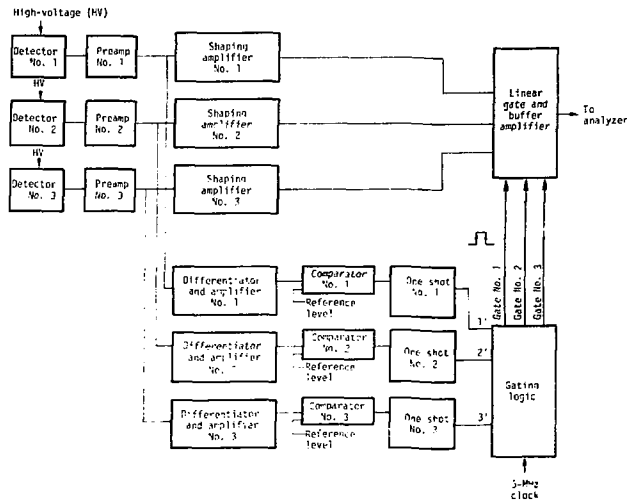


Fig. 3. Block diagram of the system electronics.

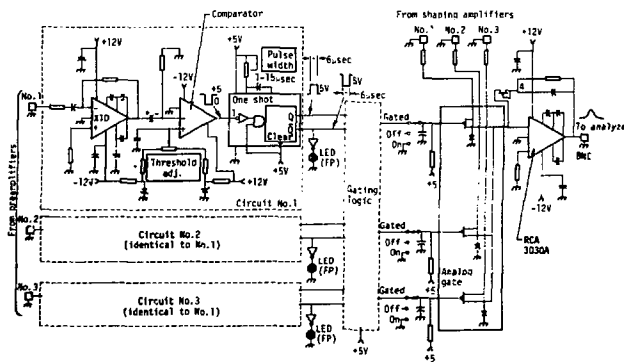


Fig. 4. Schematic of the system electronics, excluding the gating logic.

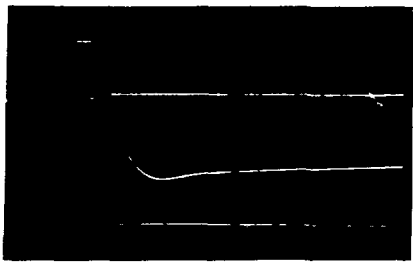


Fig. 5. Timing relationships. Top, one-shot and logic output pulse. Middle, detector signal from shaping amplifier. Bottom, gated detector signal to analyzer.

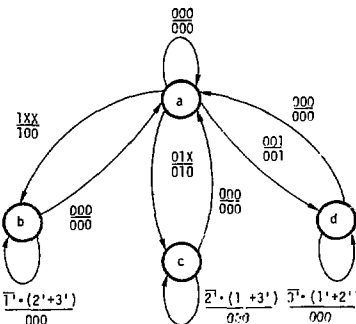


Fig. 7. State-to-state diagram for the gating sequential logic. Each directional arrow is labeled with the 1' 2' 3' input condition to the "D" flip-flops, over the 1 2 3 output condition to the linear gates; "on" is designated by 1, "off" by 0, and "don't care" by X.

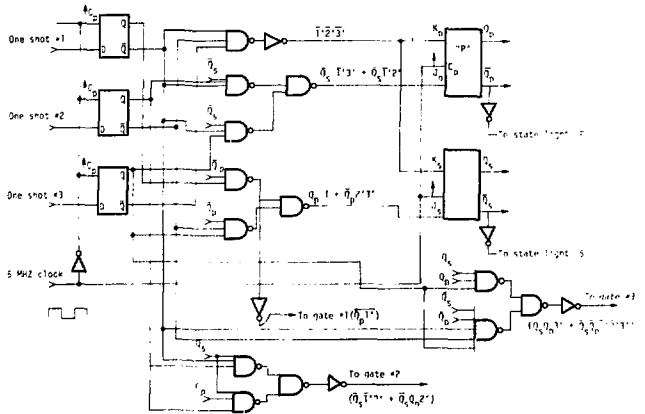


Fig. 6. Detector gating logic.

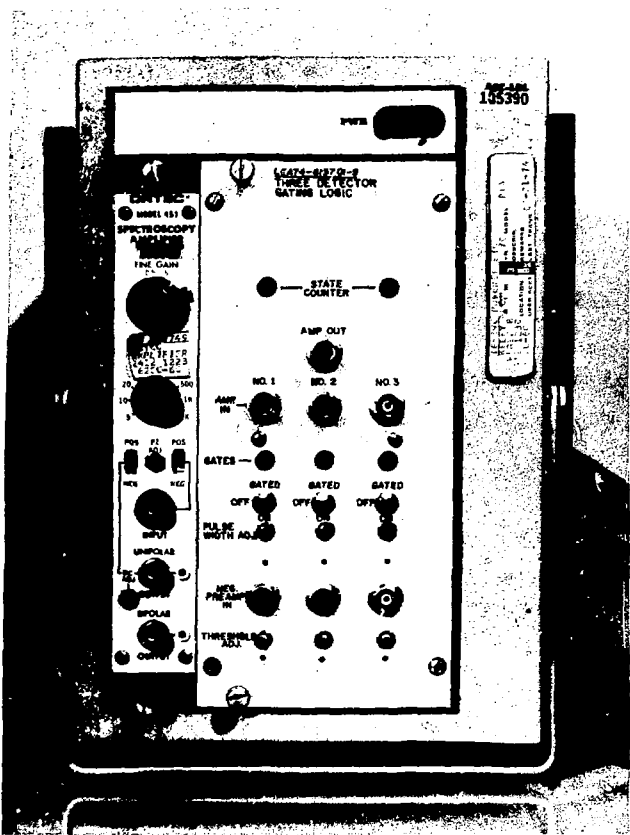


Fig. 8. Panel for the electronics of the detector gating logic.

state of the counter can be determined from two LED lights located at the top of the front panel. Also on the front panel, three lights display each one-shot output. These five lights permit a static check of the logic and have been useful in the dynamic mode to indicate the presence of a ground loop or a noise source on any of the three channels. A dynamic check of the logic can also be made by using one detector for all three channel inputs and, using the switches and a multichannel analyzer, checking each channel for the priority behavior. A  $^{241}\text{Am}$  source (60 keV) is used to set the discriminators.

Assuming that the lower-level discriminators have been previously set, the setup procedure for the system simply involves adjusting the gains of the three amplifiers to the same level and checking the gated resolution. The amplifiers use d. c. output couplings and must be adjusted to the same zero point.

### Results

The improvement in resolution of the gated mode over the summed mode, about 35%, can be seen in Fig. 9. The gated resolution at 122 keV is 3.4 keV FWHM compared to 5.3 keV FWHM in the summed mode. The improvement is in accord with the expected result, that is, the summed resolution is equal to the square root of the sum of the squares of the individual detector resolutions, and the gated resolution is approximately equal to the average resolution of the three detectors.

The peak relative efficiency at 25 cm (calculated using Heath's data<sup>1</sup>) is plotted vs. energy in Fig. 10 for both the summed and gated modes of operation. The curves peak at about 80% relative efficiency at 122 keV.

On investigation, the apparent drop in efficiency in the gated mode compared to the summed mode appeared to be due to Compton scattering between detectors. In the summed mode, if a photon causes a Compton event in one detector and is scattered to another detector, the composite sum of the detector pulses, if the absorption was completed in the detectors, is in the photopeak. Since in the gated mode output pulses are accepted from only one detector, the result will be to raise the Compton edge as seen in the spectra of the multichannel analyzer. It was determined that most of these events occur between the middle detector and one of the detectors on either side. One remedy would be to design the logic to accept coincidence pulses (within the clock period) between the center detector and one or the other of the detectors on either side. A problem could arise at high count rates, however, due to the relatively long coincidence-resolving time determined by the 4.5 MHz clock. Although at 140 keV ( $^{99}\text{Br}$ c), the percent difference in efficiency between the two modes is small, new logic has been designed for future experimentation. It should be noted here that later multi-detector systems<sup>2</sup> consisting of four thin (2.5 mm) detectors mounted edge to edge has shown no differences in efficiency between summed and gated modes. This seems to support the above explanation. The probability that Compton scattered photons will be detected by adjacent detectors is very small for these thin detectors.

The peak relative efficiency at 122 keV was found to be 93% of that of our 7.6 cm x 7.6 cm NaI(Tl) detector at 25 cm. The tumor scanner has been installed at the University of Chicago; it has

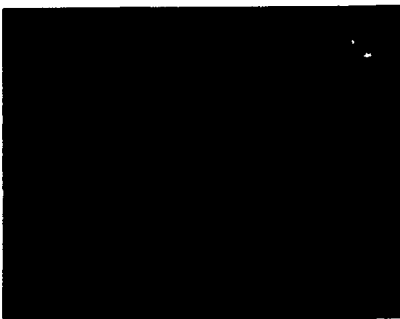


Fig. 9. Energy spectra of  $^{57}\text{Co}$ . Preamplifier outputs summed (upper) and gated (lower).

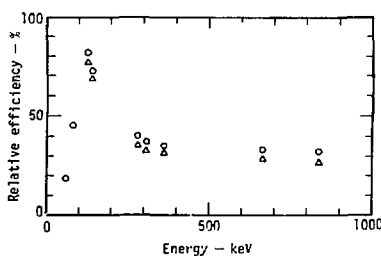


Fig. 10. The peak relative efficiencies of the University of Chicago Tumor Scanner at 25 cm in the summed mode (circles) and the gated mode (triangles).

been checked out operationally but clinical evaluation is not yet completed.

#### Conclusions

This method of detector gating should be applicable to multidetector systems where higher efficiencies are desired without the usual sacrifice in energy resolution. The number of detectors that could be paralleled by this scheme would be limited mainly by consideration of the gain stability of each amplifier and the resulting effect upon the energy resolution of the system. Because of the Compton scattering effect between detectors, consideration must be given also to their physical proximity, either in the detector mounting arrangement or in the design of the logic circuits.

#### References

1. R.L. Heath, *Scintillation Spectrometry: Gamma Ray Spectrum Catalogue*, 2nd Ed., Vol. 2 Atomic Energy Division, Idaho Operations Office, U.S. Atomic Energy Commission (AEC Research and Development Report IDO-16880-1 (1964).
2. J.A. Kirby, L.R. Anspaugh, P.L. Phelps, G.A. Armantrout, and D. Sawyer, "A detector system for in-situ spectrometric analysis of  $^{241}\text{Am}$  and Pu in soil." *IEEE Trans. Nucl. Sci.*, 1974 Nuclear Science Symposium, in press.

#### Acknowledgement

This work was performed under the auspices of the U.S. Energy Research and Development Administration Contract No. H-7405-ENG-48

"Reference to a company or product name does not imply approval or recommendation of the product by the University of California or the U.S. Energy Research & Development Administration to the exclusion of others that may be suitable."